Dalton Transactions



PAPER



Cite this: *Dalton Trans.*, 2018, **47**, 6025

R₂ (Ad = adamantyl; R = ^{neo}Pe, 1-nor) insertions and Fe-R bond dissociation enthalpies (BDEs)†‡

Dispersion forces play a role in (Me₂IPr)Fe(=NAd)

Thomas R. Cundari,*^a Brian P. Jacobs,^b Samantha N. MacMillan^b and Peter T. Wolczanski (10 * ^b

Received 2nd November 2017, Accepted 13th April 2018 DOI: 10.1039/c7dt04145d

rsc.li/dalton

The effects of dispersion on migratory insertion reactions and related iron–carbon bond dissociation energies pertaining to $(Me_2IPr)FeR_2$ (R = ^{neo}Pe , 1-nor), and the conversion of $(Me_2IPr)Fe(=NAd)R_2$ to $(Me_2IPr)Fe\{N(Ad\}R)R$ are investigated *via* calculations and structural comparisons. Dispersion appears to be an underappreciated, major contributor to common structure and reactivity relationships.

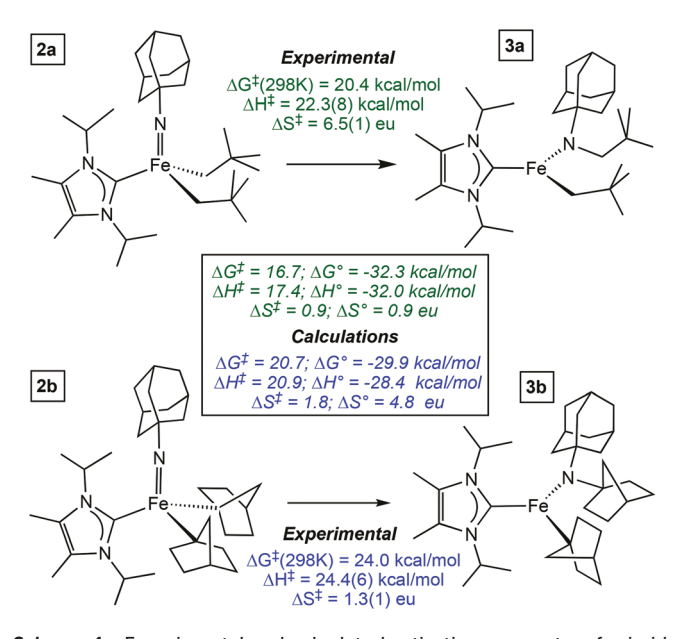
Introduction

In a recent communication, ¹ the relative rates of a rare imide insertion into a metal–carbon bond were reported. The process, which is shown in Scheme 1, is the conversion of an intermediate spin (S=1), formally iron(IV) (Me₂IPr)Fe(=NAd) R₂ (Ad = adamantyl; R = ^{neo}Pe (2a), 1-nor (2b)), generated from the corresponding dialkyls (1a,b) and adamantyl azide, to a high spin (S=2) iron(II) amide-alkyl, (Me₂IPr)Fe{N(Ad)R}R (R = ^{neo}Pe (3a), 1-nor (3b)). Calculations supporting the mechanism proved less than satisfactory unless dispersion corrections were incorporated.§

§ Complexes **1a,b**, **2a,b**, **3a,b**, ¹ and $[(1\text{-nor})\text{Li}]_4^{22,23}$ were prepared via literature methods. Amide **4b** and dialkyl **5b** were prepared as described in the text. For full experimental and calculational details, see the ESI.‡ *Crystal data for* **4b**: $\text{C}_{38}\text{H}_{52}\text{N}_4\text{Fe}$, M=620.68, monoclinic, P_{21}/c , a=10.4328(4), b=20.1032(7), c=17.3563(6) Å, $\beta=106.003(2)^\circ$, V=3499.1(2) ų, T=223(2) K, $\lambda=0.71073$ Å, Z=4, $R_{\text{int}}=0.0408$, 37447 reflections, 8039 independent, $R_1(\text{all data})=0.0589$, $wR_2=0.0949$, GOF = 1.012, CCDC-1583545.‡ *Crystal data for* **5b**: $\text{C}_{20}\text{H}_{40}P_2\text{Fe}$, M=398.31, orthorhombic, Pnma, a=18.2193(12), b=14.0581(7), c=9.3097(6) Å, V=2384.5(2) ų, T=223(2) K, $\lambda=0.71073$ Å, Z=4, $R_{\text{int}}=0.0285$, 20 682 reflections, 2271 independent, $R_1(\text{all data})=0.0467$, $wR_2=0.1282$, GOF = 1.082, CCDC-1583546.‡ *Crystal data for* [(1-nor)Li]₄: $\text{C}_{28}\text{H}_{44}\text{Li}_4$, M=408.39, monoclinic, P_{21} , a=10.3771(2), b=10.1982(2), c=11.7698(2) Å, V=1245.57(4) ų, T=100.0 (10) K, $\lambda=0.71073$ Å, Z=2, $R_{\text{int}}=0.0410$, 33 926 reflections, 5229 independent, $R_1(\text{all data})=0.0428$, $wR_2=0.1123$, GOF = 1.069, CCDC-1583544.‡

 \dagger Dedicated to Philip P. Power, synthetic chemist extraordinaire, on the occasion of his 65th birthday.

‡Electronic supplementary information (ESI) available: Experimental and calculational details, and spectroscopic information. CCDC 1583544–1583546. For ESI and crystallographic data in CIF or other electronic format see DOI: 10.1039/c7dt04145d



Scheme 1 Experimental and calculated activation parameters for imide insertions, and calculated ΔG° , ΔH° and ΔS° .

Power *et al.*² have suggested that dispersion is a crucial stabilization factor in congested, and low coordinate transition metal compounds.³ For example, dispersion forces are thought to provide favorable interligand energies in $M(1-nor)_4$ (M = Fe, 45.9 kcal mol^{-1} ; Co, 38.3 kcal mol^{-1})² as inferred from calculations of 1-nor homolysis. Fürstner has attributed the modest stability of $Fe(^cHex)_4$ in part to similar forces. As a consequence, it is worth investigating the importance of dispersion^{5–7} in bond homolysis, and related contributions to other unimolecular processes,^{8,9} such as migratory insertion.

^aDepartment of Chemistry, CASCaM, University of North Texas, Denton, Texas 76201, USA

^bDepartment of Chemistry and Chemical Biology, Baker Laboratory, Cornell University, Ithaca, NY 14853, USA. E-mail: ptw2@cornell.edu, Thomas.Cundari@unt.edu

Paper Dalton Transactions

In assessing the insertion reactions illustrated in Scheme 1 νia calculations, the more favorable enthalpy of converting $2a \rightarrow 3a \ (\Delta H^{\circ} = -32.0 \text{ kcal mol}^{-1}) \nu s. \ 2b \rightarrow 3b \ (-29.9 \text{ kcal mol}^{-1})$ translates into a lower barrier (17.4 $\nu s. \ 20.9 \text{ kcal mol}^{-1}$). What is the origin of the greater driving force that leads to faster rates for R = neopentyl $\nu s. \ R = 1$ -norbornyl?

Calculations (Table 1) on the homolysis of the iron-alkyl bonds suggested that the difference between the Fe(IV)-R and Fe(II)-R species were significantly greater for R = $^{\text{neo}}$ Pe ($\Delta\Delta H^{\circ}$ = -17.3 kcal mol^{-1}) ν s. R = 1-nor ($\Delta\Delta H^{\circ}$ = -12.0 kcal mol^{-1}). Note that the primary difference was in the Fe(IV) species, **2a** ν s. **2b**, where the 1-norbornyl derivative was calculated to have a 7.0 kcal mol^{-1} greater bond dissociation enthalpy (BDE), whereas it was only calculated to be 1.7 kcal mol^{-1} stronger in the ferrous product, **3a** ν s. **3b**. Herein it is suggested that dispersion plays a significant role in the BDE disparity, and other structural comparisons support the importance of dispersion.

Results and discussion

Reaction coordinates

Prior to assessing factors that address BDEs, it is important to determine whether a simple insertion reaction coordinate (RC) that has substantial iron–carbon bond breaking is reasonable. Using metric parameters and energies of the ground states (GSs) and transition states (TSs) supplied by the calculations, a RC consisting of the N(imide) to alkyl distance was explored. Fig. 1 illustrates the (Me₂IPr)Fe(=NAd)(^{neo}Pe)₂ (2a) insertion process to afford (Me₂IPr)Fe{N(Ad)^{neo}Pe}^{neo}Pe (3a), using parabolic enthalpy surfaces. Intersystem crossing from the GS triplet of 2a to its corresponding quintet surface, *prior* to the transition state of insertion, is in accord with the calculation of a lower lying quintet TS.¹ As a consequence, a straightforward RC of Fe–C(^{neo}Pe) bond-breaking and N–C(^{neo}Pe) bond making is deemed reasonable. The transition state is characterized by an imaginary frequency at 303 cm⁻¹.

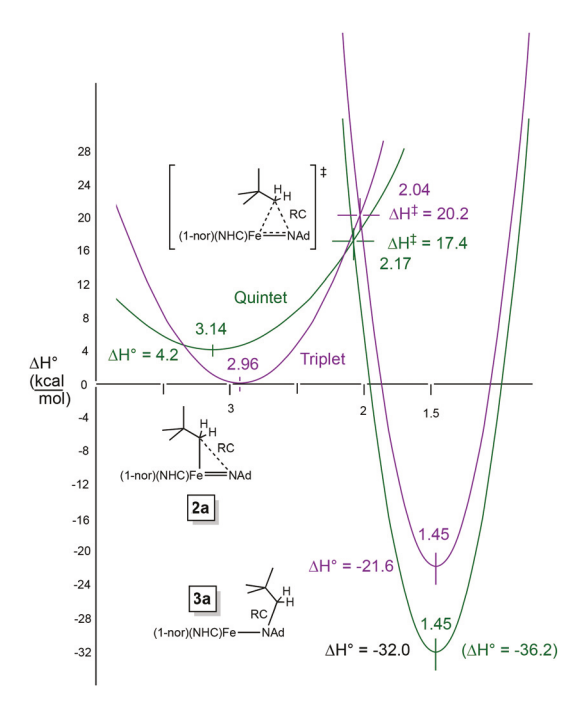


Fig. 1 Parabolic fit of metric parameters and enthalpies pertaining to the insertion reaction: $(Me_2IPr)Fe(=NAd)(^{neo}Pe)_2$ (2a) \rightarrow $(Me_2IPr)Fe(NAd)^{neo}Pe)^{neo}Pe$ (3a); x-axis is d(NC) = RC as per dashed lines.

Fig. 2 illustrates the related parabolic diagram pertaining to the insertion of the 1-norbornyl derivative: $(Me_2IPr)Fe(=NAd)$ $(1-nor)_2$ $(2b) \rightarrow (Me_2IPr)Fe\{N(Ad)(1-nor)\}(1-nor)$ (3b). Once again, the migratory insertion path faithfully reproduces an intersystem crossing event from the triplet to quintet 2b surfaces that occurs before the transition state. The 285 cm^{-1} imaginary frequency that characterizes the TS is consistent with its higher energy with respect to that of the $^{\text{neo}}Pe$ case. It is likely that the quintet TS of the $2a \rightarrow 3a$ system has greater triplet character due to its closer energy to the intersystem crossing event. Greater mixing in this $^{\text{neo}}Pe$ case can also contribute to the higher frequency relative to the 1-nor system.

Table 1 Calculated (with and without dispersion) ground state BDEs and BDFEs for the homolytic dissociation of R ([Fe] = $(Me_2|Pr)Fe$) in kcal mol⁻¹

Iron alkyl species	$BDE^{a}(w)$	$\mathrm{BDE}^b\left(\mathrm{w/o}\right)$	Δ^c	$BDFE^{a}$ (w)	$\mathrm{BDFE}^b\left(\mathrm{w/o}\right)$	Δ^c
[Fe](^{neo} Pe) ₂ (1a)	51.1	34.8	16.3	35.5	21.7	13.8
$[Fe](1-nor)_2(1b)$	57.0	36.0	21.0	42.2	24.0	18.2
$[Fe](=NAd)(\stackrel{\text{neo}}{=}Pe)_2$ (2a, S = 1)	36.5^{d}	13.6^{d}	22.9^{d}	18.1^{d}	-4.1^{d}	22.2^{d}
(2a, S = 3)	32.3^{e}	11.4^e	20.9^{e}	15.2^{e}	-4.5^{e}	19.7 ^e
$[Fe](=NAd)(1-nor)_2 (2b, S = 1)$	43.5^{d}	16.7^{d}	26.8^{d}	26.0^{d}	-0.8^{d}	26.8^{d}
(2b, S = 3)	39.5^{e}	15.6^{e}	23.9^{e}	24.0^{d}	-0.2^{e}	24.2^{e}
$[Fe]{N(Ad)^{n\acute{e}o}Pe}(^{neo}Pe)$ (3a)	53.8	37.0	16.8	36.2	22.0	14.2
[Fe]{N(Ad)(1-nor)}(1-nor) (3b)	55.5	35.5	20.0	41.2	21.8	19.4
$[Fe]{N(NCPh_2)(1-nor)}(1-nor)(4b)$	49.6	29.9	19.7	34.5	16.5	18.0
$2\mathbf{a}\left(S=1\right)\to 3\mathbf{a}\left(S=1\right)^f$	-17.3^{d}	-23.4^{d}		-18.1^{d}	-26.1^{d}	
	-21.5^{e}	-25.6^{e}		-21.0^{e}	-26.5^{e}	
2b $(S = 1) \rightarrow 3b (S = 1)^f$	-12.0^{d}	-18.8^{d}		-15.2^{d}	-22.6^{d}	
	-16.0^{e}	-19.9^{e}		-17.2^{e}	-22.0^{e}	

^a B3PW91-GD3/G-31+G(d) w/dispersion. ^b B3PW91/G-31+G(d) without dispersion. ^c Δ = Δ BDE = BDE(w/disp) – BDE; Δ = Δ BDFE = BDFE(w/disp) – BDFE. ^d Triplet GS. ^e Quintet excited state (ES, *italicized*). ^f Δ Δ*H* and Δ Δ*G* values for the conversion described.

Dalton Transactions Paper

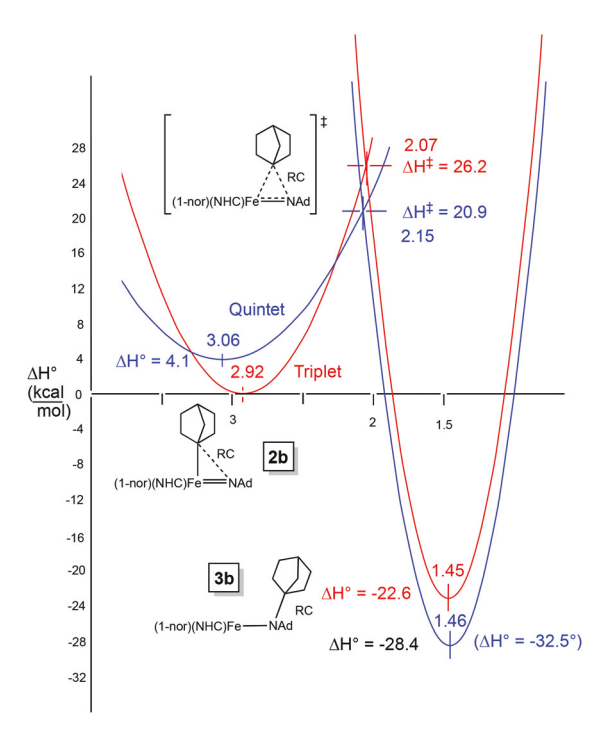


Fig. 2 Parabolic fit of metric parameters and enthalpies pertaining to the insertion reaction: $(Me_2|Pr)Fe(=NAd)(1-nor)_2$ (2b) \rightarrow $(Me_2|Pr)Fe\{N(Ad)(1-nor)\}(1-nor)$ (3b); x-axis is d(NC) = RC as per dashed lines.

Factors influencing insertion rates via BDEs

Now that the reaction coordinate has been explored and is shown to be consistent with elements of Fe–C bond breaking, factors that influence the BDEs of the two systems can be analyzed. Experimental carbon–hydrogen bond energies for neoPe–H and (1-nor)H are 100.3 (99.4 (calc)) and 96.7 (104.2 calc; 105.5 (G4 *ab initio*)) kcal mol⁻¹, respectively. 10 The (1-nor) H BDE is somewhat higher than expected (*e.g.*, Me₃CH, BDE = 95.7 kcal mol⁻¹, 92.1 calc, 96.0 (G4 *ab initio*)) due to the "tied-back" nature of the tertiary carbon on norbornane, which imparts slightly more s-character (26% *vs.* 22% in isobutane) to the bridgehead position. The experimental C–H BDEs suggest that corresponding Fe–C(^{neo}Pe) bonds should be stronger than the Fe–C(1-nor) interactions, 11-13 but calculations do not support this statement.

A perusal of the calculated BDEs and BDFEs (bond dissociation free energies) in Table 1 shows that the 1-norbornyl derivatives are greater than the neopentyl cases in all three compound types: $(Me_2IPr)FeR_2$ (1), $(Me_2IPr)Fe(=NAd)R_2$ (2), and $(Me_2IPr)Fe\{N(Ad)(R)\}R$ (3). More importantly, dispersion contributes a substantial amount to the stabilization of all of these complexes. For example, the BDEs (without dispersion) for the Fe(IV) (2) species indicate that the complexes would be unstable if not for contributions due to dispersion.

The aforementioned linear free energy relationship that is believed responsible for the faster rate of $2a \rightarrow 3a \ \nu s$. $2b \rightarrow 3b$ originates in the calculated BDE difference (5.3 kcal mol⁻¹) between the Fe(IV)–R and Fe(II)–R species: R = $^{\text{neo}}$ Pe, $\Delta \Delta H^{\circ}$ =

-17.3 kcal mol⁻¹; R = 1-nor, $\Delta\Delta H^\circ$ = -12.0 kcal mol⁻¹. When dispersion is removed from the calculations, the neopentyl case is still favored by slightly less (4.6 kcal mol⁻¹). Differences in dispersion factors are slightly greater between the Fe(ν) derivatives, where the iron–carbon bond strengths are 7.0 kcal mol⁻¹ stronger for **2b** ν s. **2a**; they are only 1.7 stronger for **3b** ν s. **3a**. BDE calculations without dispersion show only a 3.1 kcal mol⁻¹ difference, and the D(FeC) in **3a** is actually 1.5 kcal mol⁻¹ stronger than in **3b**. Given these results, it is also quite plausible that the experimental BDEs on (1-nor)H are not viable.

In summary, dispersion forces account for 31–37% of the BDE for the three-coordinate (Me₂IPr)FeR₂ (1) and (Me₂IPr)Fe {N(Ad)(R)}R (3) species, and 62–63% of the BDE in the more sterically congested four coordinate imido complexes, (Me₂IPr) Fe(=NAd)R₂ (2). The influence of dispersion is greater for the 1-norbornyl complexes, and the slower rate of insertion for the 1-nor case (2b \rightarrow 3b) νs . the ^{neo}Pe system is subtly impacted by this difference.

(Me₂IPr)Fe{N(N=CPh₂)(1-nor)}(1-nor): synthesis, structure and calculation

Common to both insertion processes is the adamantyl group attached to the imide in $(Me_2IPr)Fe(=NAd)R_2$ ($R = ^{neo}Pe$ (2a), 1-nor (2b)), and the amide in $(Me_2IPr)Fe\{N(Ad)R\}R$ ($R = ^{neo}Pe$ (3a), 1-nor (3b)). While no other Fe(IV) imides proved stable enough to provide an experimental comparison, treatment of $(Me_2IPr)Fe(1-nor)_2$ with $Ph_2CN_2^{14-17}$ did provide another Fe(II) amide complex, $(Me_2IPr)Fe\{N(N=CPh_2)(1-nor)\}(1-nor)$ (4b, 57%), according to eqn (1). No intermediates were detected, as the solution merely darkened from light-yellow to orangebrown, consistent with transient imide formation and rapid insertion. The μ_{eff} , conducted via Evans' method, 18 was $4.7\mu_B$, consistent with an S = 2 center.

$$(Me_2I Pr)Fe(1 - nor)_2 + Ph_2CN_2 \xrightarrow{23 \, {}^{\circ}C, \, 1 \, h, \, C_6H_6}$$

$$(Me_2I Pr)Fe\{N(N = CPh_2)(1-nor)\}(1-nor)(4\mathbf{b})$$

$$(1)$$

Fig. 3 illustrates a molecular view of $(Me_2IPr)Fe\{N(N=CPh_2)(1-nor)\}\{(1-$

Calculations of the iron–1-norbornyl bond dissociation energy and free energy pertaining to $(Me_2IPr)Fe\{N(N=CPh_2)(1-nor)\}(1-nor)$ (4b) afford slightly smaller values than that of $(Me_2IPr)Fe\{N(Ad)(1-nor)\}(1-nor)$ (3b). Differences in BDE calculated with and without dispersion ($\Delta BDE = 19.7$ kcal mol^{-1}) are essentially the same as in 3b. The system has other components that do not permit a ready comparison of adamantyl

Paper Dalton Transactions

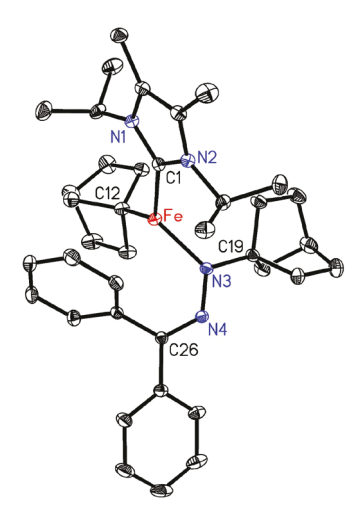


Fig. 3 Molecular view of $(Me_2lPr)Fe\{N(N=CPh_2)(1-nor)\}(1-nor)$ (4b). Interatomic distances (Å) and angles (°): Fe-N3, 2.0023(14); Fe-C1, 2.1450(16); Fe-C12, 2.0780(17); N3-N4, 1.3521(18); N4-C26, 1.305(2); N3-C19, 1.457(2); N3-Fe-C12, 113.41(6); N3-Fe-C1, 117.91(6); C1-Fe-C12, 123.96(6); Fe-N3-N4, 128.29(10); Fe-N3-C19, 119.90(10); N3-N4-C26, 121.57(14).

vs. Ph₂C=N group effects, especially since the likely imide precursor was not observed.

(Me₃P)Fe(1-nor)₂: synthesis, structure and isodesmic calculation

In Power's initial study of the impact of dispersion on $Fe(1-nor)_4$, an isodesmic calculation was used to show the effect on an equilibrium with "FeH₄". In order to corroborate these findings, and those of the preceding 1-norbornyl derivatives, a related isodesmic reaction was calculated. First, treatment of $(Me_3P)_2FeCl_2$ with 2 equiv. of (1-nor)Li producted off-white $(Me_3P)_2Fe(1-nor)_2$ (5b) in 61% yield.

$$\begin{aligned} \left(Me_{3}P\right)_{2}FeCl_{2} + 2Li(1\text{-nor}) &\xrightarrow{23\,^{\circ}C,\,1\,h,\,C_{6}H_{6}} \left(Me_{3}P\right)_{2}Fe(1\text{-nor})_{2}(\textbf{5b}) \end{aligned} \tag{2}$$

Evans' method¹⁸ measurements of **5b** gave a μ_{eff} of 4.7 μ_{B} , consistent with a pseudo tetrahedral S = 2 system.

Despite severe rotational disorders in the 1-norbornyl and PMe₃ ligands, a reasonable structural model for $(Me_3P)_2Fe(1-nor)_2$ (5b) was obtained *via* X-ray crystallography, and a molecular view is illustrated in Fig. 4. The C–Fe–C angle pertaining to the 1-nor groups is $120.32(12)^\circ$, while the phosphorus atoms are $99.53(4)^\circ$ apart, and all remaining core angles are $108.75(29)^\circ$. The bond distances of 2.057(2) and 2.410(4) Å pertaining to d(Fe-C) and d(Fe-P), respectfully, are normal for tetrahedral ferrous species.

Fig. 5 shows the isodesmic reaction of Fe(1-nor)₄ and $(Me_3P)_4$ Fe comproportionating to two equiv. of $(Me_3P)_2$ Fe(1-nor)₂ (5b). First, note that $(Me_3P)_4$ Fe actually exists as $(Me_3P)_3$ HFe(η^2 -CH₂PMe₂),²⁰ but its reactivity is akin to the iron(0) tetrakis-phosphine species, and is thus considered close in energy. Depending on the levels of theory utilized, dispersion accounts for ~15 kcal mol⁻¹ of enthalpic stabilization

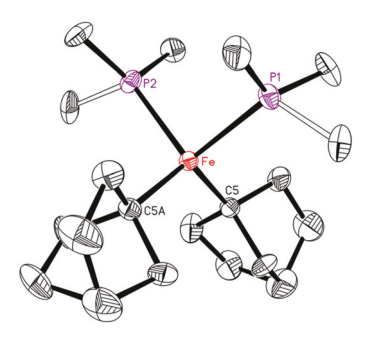


Fig. 4 Molecular view of highly disordered $(Me_3P)_2Fe(1-nor)_2$ (5b). Interatomic distances (Å) and angles (°): Fe-C5, 2.057(2); Fe-P1, 2.4127(10); Fe-P2, 2.4076(9); C5-Fe-C5A, 120.32(12); C5(C5A)-Fe-P2, 108.50(7); C5(C5A)-Fe-P1, 109.00(6); P1-Fe-P2, 99.53(4).

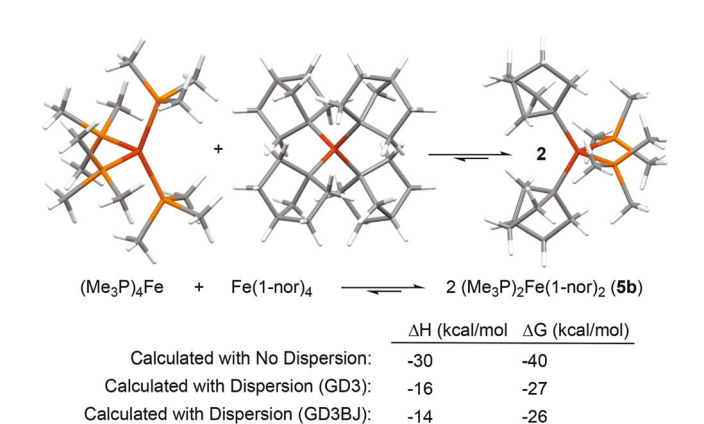


Fig. 5 Calculated ΔH and ΔG for the comproportionation of $(Me_3P)_4Fe + Fe(1-nor)_4$ to 2 $(Me_3P)_2Fe(1-nor)_2$ (5b) with and without corrections due to dispersion.

in the homoleptic complexes, mostly in Fe(1-nor)₄. The six (1-nor)/(1-nor) interactions on the reactant side are offset by two in the products, one for each 5b. While the magnitude per 1-nor ligand is less than claimed for Fe(1-nor)₄ alone,² these results – all on known, isolable (or isomeric in the case of $(Me_3P)_4Fe$) complexes – support the contention that dispersion plays a crucial role in low coordinate complexation. The lower values are undoubtedly due to the fact that dispersion via the PMe₃ ligands contributes substantially, albeit at longer distances due to the d(Fe-P) being ~ 0.35 Å longer than the d(Fe-C).

Note that the comproportionation of Fe(0) and Fe(IV) to two equiv. Fe(II) is favorable in the isodesmic calculation above, in contrast to the synthesis of Fe(1-nor)₄, 21,22 which is prepared from (1-nor)Li and Fe(II) sources in weakly donating solvents. Theopold's related studies on $[Co(1-nor)_4]^n$ (n=-1, 0, +1)²³ helped show that disproportionation to M(IV) and M(0) is the likely path for iron and cobalt. The maximization of dispersion is a plausible factor enabling formation of the M(IV) species, but if a significant donor ligand is also present, as in the PMe₃ case above, iron(II) persists as the stable form. Presumably, favoring Fe(II)²⁴ entails both ligand donor interactions as well as, at least in the case of PMe₃, additional dispersion factors.

Dalton Transactions Paper

[(1-nor)Li]₄: structure and isodesmic calculation

The use of the 1-nor group to stabilize tetrahedral $M(1-nor)_4$ transition metal complexes, and its high degree of covalence in the corresponding high formal oxidation state metal-carbon bonds, prompted a structural study of Li(1-nor) aggregates.

Crystallization of (1-nor)Li^{23,25} from pentane solvent afforded a tetramer, whose structure is illustrated in Fig. 6. The lithium atoms are disposed in a regular tetrahedron, with d(Li-Li) = 2.419(17) Å (ave). The α -carbons of each 1-norbornyl unit are equidistant to each Li₃ face, with $d(\text{C}(\alpha)\text{-Li}) = 2.206(16)$ Å (ave). Interactions of the β -carbons with the lithium atoms range from 2.3 to 3.6 Å.

Fig. 7 depicts the gas phase dimerization of $[(1-\text{nor})\text{Li}]_2$ and tetramerization of (1-nor)Li to tetrahedral $[(1-\text{nor})\text{Li}]_4$ with associated enthalpies calculated with and without dispersion. Assuming six (1-nor)/(1-nor) interactions in the tetramer, dispersion accounts for $\sim 30-40$ kcal mol^{-1} , or roughly 6–8 kcal mol^{-1} per interaction relative to 4 (1-nor)Li. The amount of dispersive energy in each aggregation is method dependent with the GD3BJ correction giving the higher values.

Since the bonding of each RLi fragment differs in the monomer and each aggregate, it is imperative to compare the

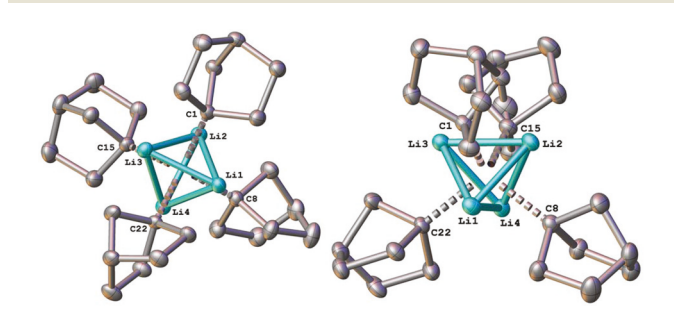


Fig. 6 Two molecular views of tetrameric [(1-nor)Li]₄. Interatomic distances (Å) and angles (°): Li1-C1, 2.213(5); Li-C8, 2.190(5); Li1-C22, 2.219(5); Li2-C1, 2.225(5); Li2-C8, 2.217(5); Li2-C15, 2.190(5); Li3-C1, 2.193(5); Li3-C15, 2.230(5); Li3-C22, 2.217(5); Li4-C8, 2.190(5); Li4-C15, 2.198(5); Li4-C22, 2.189(5); Li-Li, 2.419(17) (ave).

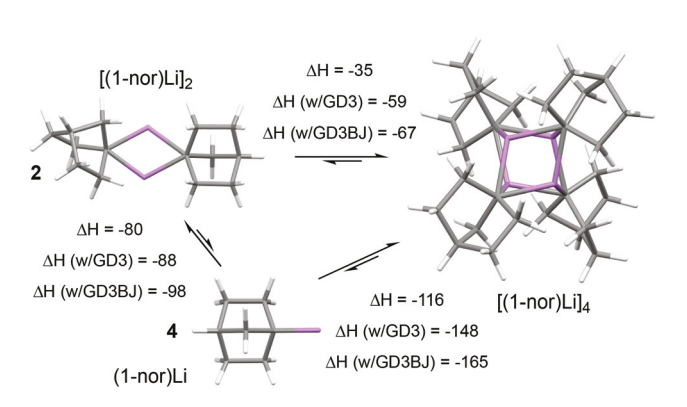


Fig. 7 ΔH (kcal mol⁻¹) for tetramerization and dimerization of (1-nor)Li and [(1-nor)Li]₂ to [(1-nor)Li]₄, calculated without and with (GD3, GD3BJ) dispersion.

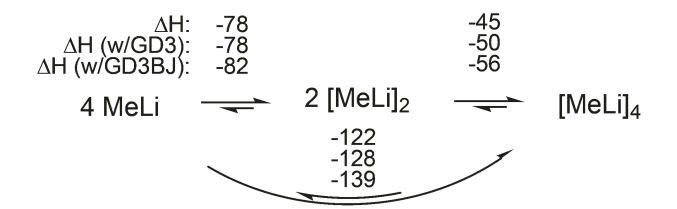


Fig. 8 ΔH (in kcal mol⁻¹) for tetramerization and dimerization of MeLi and [MeLi]₂ to [MeLi]₄, calculated without and with (GD3, GD3BJ) dispersion.

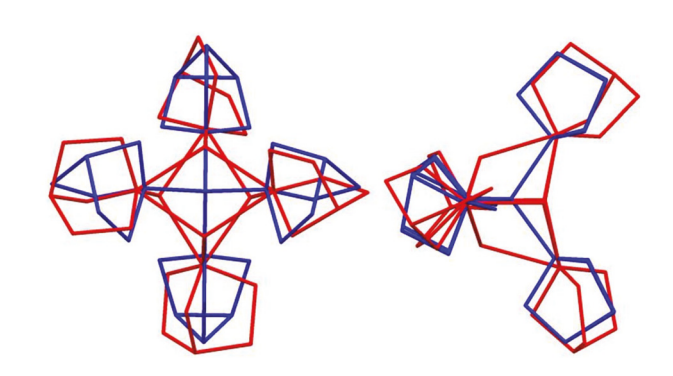


Fig. 9 Wireframe views of the superposition of Fe(1-nor)₄ (blue) and [(1-nor)Li]₄, clearly showing structurally related 1-norbornyl groups, which likely lead to similar dispersion interactions.

 $[(1-\text{nor})\text{Li}]_n$ systems with one in which a significantly smaller amount of dispersion is likely. Fig. 8 illustrates the related case of MeLi aggregation, which manifests similar enthalpic changes, but less correction from dispersion. Even for the tetramerization of MeLi, dispersion contributes 6–17 kcal mol⁻¹, whereas the corresponding tetramerization of (1-nor)Li has a corresponding 32–49 kcal mol⁻¹. It is noteworthy that such corrections appear important even for small RLi.

Conclusions

According to the calculations herein, there is no question that dispersion is consequential to structural stability. As an enthalpic contribution, chemical reactivity and affiliated rates can also be affected. The magnitude of these effects is surprising, especially the realization that simple bond dissociation enthalpies can have a substantial dispersion component.

The results above, prompted by the observations of Power *et al.*, ²⁻⁴ show that the forces of dispersion have been underappreciated in areas outside of solvation and materials. ^{26,27} Consider the structures of Fe(1-nor)₄ and [(1-nor)Li]₄ illustrated in Fig. 9. It appears reasonable that the same force is critical in holding these disparate species to their tetrahedral geometries, and that force is likely to be dispersion.

This work also serves to highlight dispersion as a force that needs to be considered in systems featuring large hydrocarbons. It must be emphasized that the magnitudes of dispersion factors, while a point of emphasis in this research, Paper Dalton Transactions

should be appreciated as method dependent. The model used herein was introduced by Power, Nagase, and coworkers, ^{2,9} and was chosen for comparison. It is also important to recognize that gas phase calculations are utilized herein, and solvation dispersion forces, say in stabilizing the fragments of homolytic bond dissociation, may impact interpretations. Recent evidence supports the contention that ligand/substrate dispersion interactions play crucial roles in catalytic selectivities.²⁸

Conflicts of interest

There are no conflicts to declare.

Acknowledgements

We gratefully acknowledge financial support of the NSF (PTW: CHE-1664580; Cornell NMR Facility, CHE-1531632. TRC: CHE-1531468 (CASCaM)), and the DOE (TRC: DE-FG02-03ER15387).

Notes and references

- B. P. Jacobs, P. T. Wolczanski, Q. Jiang, T. R. Cundari and S. N. MacMillan, J. Am. Chem. Soc., 2017, 139, 12145–12148.
- 2 D. J. Liptrot, J. D. Guo, S. Nagase and P. P. Power, *Angew. Chem.*, *Int. Ed.*, 2016, 55, 14766–14769.
- 3 D. J. Liptrot and P. P. Power, Nat. Rev. Chem., 2017, 1, 0004.
- 4 A. Casitas, J. A. Rees, R. Goddard, E. Bill, S. DeBeer and A. Fürstner, *Angew. Chem., Int. Ed.*, 2017, **56**, 10108–10113.
- 5 J. P. Wagner and P. R. Schreiner, *Angew. Chem., Int. Ed.*, 2015, **54**, 12274–12296.
- 6 J. P. Wagner and P. R. Schreiner, *J. Chem. Theory Comput.*, 2016, **12**, 231–237.
- 7 S. Rösel, H. Quanz, C. Logemann, J. Becker, E. Mossou, L. Cañadillas-Delgado, E. Caldeweyher, S. Grimme and P. R. Schreiner, J. Am. Chem. Soc., 2017, 139, 7428–7431.
- 8 (*a*) S. Grimme and J.-P. Djukic, *Inorg. Chem.*, 2010, **49**, 2911–2919; (*b*) S. Grimme and J.-P. Djukic, *Inorg. Chem.*, 2011, **50**, 2619–2628.

- (a) C.-Y. Lin, J.-D. Guo, J. C. Fettinger, S. Nagase, F. Grandjean, G. J. Long, N. F. Chilton and P. P. Power, *Inorg. Chem.*, 2013, 52, 13584–13593; (b) C. L. Wagner, L. Tao, E. J. Thompson, T. A. Stich, J. Guo, J. C. Fettinger, L. A. Berben, R. D. Britt, S. Nagase and P. P. Power, *Angew. Chem.*, *Int. Ed.*, 2016, 55, 10444–10447.
- 10 Handbook of Bond Dissociation Energies in Organic Compounds, ed. Y.-R. Luo, CRC Press, New York, 2003.
- 11 J. L. Bennett, T. P. Vaid and P. T. Wolczanski, *Inorg. Chim. Acta*, 1998, **270**, 414–423.
- 12 H. E. Bryndza, L. K. Fong, R. A. Paciello, W. Tam and J. E. Bercaw, J. Am. Chem. Soc., 1987, 109, 1444–1456.
- 13 Y. Jiao, M. E. Evans, J. Morris, W. W. Brennessel and W. D. Jones, *J. Am. Chem. Soc.*, 2013, 135, 6994–7004.
- 14 W. A. Herrmann, Angew. Chem., Int. Ed. Engl., 1978, 17, 800–812.
- 15 T. M. Trnka and R. H. Grubbs, Acc. Chem. Res., 2001, 34, 18–29.
- 16 M. Dartiguenave, M. J. Menu, E. Deydier, Y. Dartiguenave and H. Siebald, *Coord. Chem. Rev.*, 1998, **178**, 623–663.
- 17 N. D. Harrold, A. R. Corcos and G. L. Hillhouse, *J. Organomet. Chem.*, 2016, **813**, 46–54.
- 18 (a) D. F. Evans, *J. Chem. Soc.*, 1959, 2003–2005; (b) E. M. Schubert, *J. Chem. Educ.*, 1992, **69**, 62.
- 19 H. H. Karsch, Chem. Ber., 1977, 110, 2222-2235.
- 20 H. H. Karsch, H.-F. Klein and H. Schmidbaur, *Chem. Ber.*, 1977, **110**, 2200–2212.
- 21 B. K. Bower and H. G. Tennent, *J. Am. Chem. Soc.*, 1972, **94**, 2512–2514.
- 22 R. A. Lewis, B. E. Smiles, J. M. Darmon, S. C. E. Stieber, G. Wu and T. W. Hayton, *Inorg. Chem.*, 2013, 52, 8218– 8227.
- 23 E. K. Byrne and K. H. Theopold, *J. Am. Chem. Soc.*, 1989, 111, 3887–3896.
- 24 P. T. Wolczanski, Organometallics, 2017, 36, 622-631.
- 25 H. B. Abrahamson, K. L. Brandenburg, B. Lucero and M. E. Martin, *Organometalllics*, 1984, 3, 1379–1386.
- 26 J. Hermann, R. A. DiStasio Jr. and A. Tkatchenko, *Chem. Rev.*, 2017, 117, 4714–4758.
- 27 A. Ambrosetti, N. Ferri, R. A. DiStasio Jr. and A. Tkatchenko, *Science*, 2016, 351, 1176.
- 28 G. Lu, R. Y. Liu, Y. Yang, C. Fang, D. S. Lambrecht and S. L. Buchwald, *J. Am. Chem. Soc.*, 2017, **139**, 16548–16555.